



## A FAMILY OF NEW GENERATION MINIATURIZED IMPEDANCE ANALYZERS FOR TECHNICAL OBJECT DIAGNOSTICS

Jerzy Hoja, Grzegorz Lentka

Gdansk University of Technology, Faculty of Electronics Telecommunications and Informatics, Gabriela Narutowicz 11/12, 80-233 Gdańsk, Poland (✉ hoja@eti.pg.gda.pl, +48 58 347 1487, lentka@eti.pg.gda.pl)

### Abstract

The paper presents the family of three analyzers allowing to measure impedance in the range of  $10 \Omega < |Z_x| < 10 \text{ G}\Omega$  in a wide frequency range from 10 mHz up to 100 kHz. The most important features of the analyzer family are: miniaturization, low power consumption, low production cost, telemetric controlling and the use of an impedance measurement method based on digital signal processing (DSP). The miniaturization and other above-mentioned features of the analyzers were obtained thanks to the use of the newest generation of large-scale integration chips: e.g. “system on a chip” microsystems (AD5933), 32-bit AVR32-family microcontrollers and specialized modules for wireless communication using the ZigBee standard. When comparing metrological parameters, the developed instrumentation can equal portable analyzers offered by top worldwide manufacturers (Gamry, Ivium) but outperforms them on smaller dimensions, weight, a few times lower price and the possibility to work in a distributed telemetric network. All analyzer versions are able to be put into medium-volume production.

Keywords: technical object diagnostics, impedance spectroscopy, impedance analyzer.

© 2013 Polish Academy of Sciences. All rights reserved

### 1. Introduction

Impedance spectroscopy is an advanced research tool, widely used in science [1], technique [2, 3] and medicine [4, 5] for evaluation of state or quality and diagnosis of technical and biological objects. It relies on vector impedance measurement performed in a wide frequency range from mHz up to MHz. The obtained impedance spectrum, presented in Bode or Nyquist plots, allows parametric identification of many different objects, which can be modeled by an electrical equivalent circuit, using model fitting to experimental data method (CNLS [6, 7]).

Wide, continuously growing, usage of impedance spectroscopy implies growing needs for impedance analyzers, especially low-cost and field-worthy ones. The offer of big companies in this range is not satisfying and has gaps. Till now, leading companies: Solartron, Agilent, Novocontrol, Zahner have manufactured laboratory analyzers (e.g. FRA1260 [8], Agilent4294A [9], ALPHA [10]) which were rather expensive (above 20 000 EUR). In the last years, a cheaper, portable, able to work in the laboratory as well as directly in the field, instrumentation has been proposed. Two worldwide manufacturers: American Gamry (Gamry Reference 600 [11]), Dutch Ivium (Ivium Compact Stat[12]) and one national: Atlas-Sollich (Atlas 0441 [13]) have started production.

When analyzing the worldwide market of impedance spectroscopy instrumentation and comparing it to a wide range of possible applications of impedance spectroscopy, it can be noticed that the nowadays portable impedance analyzers do not fulfil the current requirements neither functionally nor costly or dimensionally, especially in case of tests performed directly

in the field, including multi-point telemetric measurements. This leads to the conclusion that there is a need for miniaturized, low-cost and field-worthy impedance analyzers. The new family of impedance analyzers presented in the paper answers the existing needs.

## 2. Anticorrosion coating spectroscopy

Evaluation of anticorrosion coatings is the most important application area of impedance spectroscopy in economy, due to huge losses caused by corrosion. Impedance spectroscopy allows to determine protective properties of coating on objects located directly in the field, *e.g.* on bridges, pipelines, high-voltage pylons (Fig. 1), in order to decide whether the coating is in good condition or in a bad state requiring renovation [14]. The coating impedance measurement is performed in the area limited by a measurement cell filled with 3% water solution of NaCl, between a platinum electrode located in the cell and metal surface protected by the anticorrosion coating.

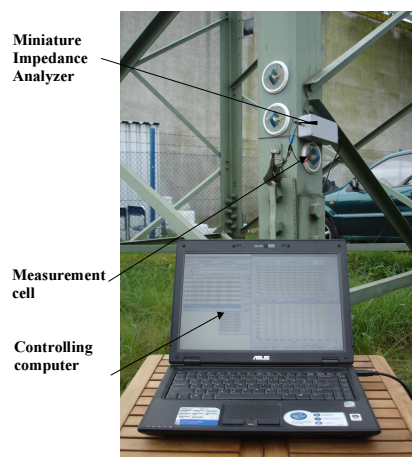


Fig. 1. Paint coating impedance measurement using a miniature impedance analyzer on the high-voltage pylon.

If the coating is new and there is no coating penetration by the electrolyte, the equivalent circuit (Fig. 2) contains only two elements: capacitance  $C_c$  (of an order of tens – hundreds pF) and resistance  $R_p$  (several – hundreds  $G\Omega$ ) modeling the properties of the coating material. After some time the coating loses seal, the electrolyte starts to penetrate the coating, but still there is no undercoating rusting. At this stage, the influence of the resistance of the electrolyte in the pores on  $R_p$  becomes visible. The value of  $R_p$  decreases as more as the electrolyte penetrates the coating. Additionally, the coating electrolyte penetration causes an increase of the dielectric constant thus causing the capacitance  $C_c$  to increase. In the next stage, the coating continuity breaks and undercoating rusting begins. New components: double layer capacitance  $C_{dl}$  and charge transfer resistance  $R_{ct}$  appear in the equivalent circuit. As the corrosion continues, the value of  $R_p$  still decreases as long as the coating is destroyed.

Modern high-thickness coatings are characterized by very high impedance, so their evaluation requires impedance spectrum determination in a wide frequency range, including very low frequencies (from mHz). Repeating the impedance spectrum measurement and performing an identification of equivalent circuit components (using CNLS), the values of components  $C_{dl}$  and  $R_{ct}$  can be found to prevent the corrosion development owing to anticorrosion coating renovation.

*Metrol. Meas. Syst.*, Vol. XX (2013), No. 1, pp. 43–52.

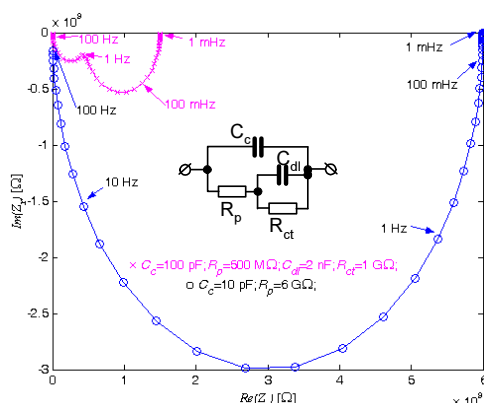


Fig. 2. The equivalent circuit and Nyquist plot of anticorrosion coating impedance in different stages of exploitation: at the initial stage (o) and at the moment of undercoating rusting appearance (x).

In order to detect the moment of undercoating rusting appearance, there is the necessity of continuous coating monitoring on the object directly in the field. This implies the need for low-cost, miniaturized, portable, field-worthy impedance analysers.

### 3. Impedance analyzer architecture

Impedance analyzers to be able to measure different objects must be characterized by the following features:

- Impedance measurement in the grounded and non-grounded equivalent circuit,
- The possibility of free-potential compensation of the electrochemical cell existing in the object under test,
- harmonic excitation with programmed amplitude and DC offset,
- analyzer powering using an USB interface or built-in accumulator battery,
- controlling by PC via wire or wireless communication.

In order to fulfil the above requirements, the Authors have developed the family of three analyzers with different features and miniaturization degrees:

1. Low-cost, miniature analyzer with wire communication, powered from controlling computer via USB, with basic features (without DC compensation and DC polarization).
2. Miniature analyzer with wire communication, powered via USB, with advanced features.
3. Wireless communication analyzer with built-in battery, designed to work in a telemetric network and testing difficult-to-reach, distributed objects in the field.

All versions of the analyzer block diagram are presented in Fig. 3.

The realized analyzer generation has been featured by new solutions:

- the use of two replaceable 2- and 3-wire impedance interfaces (2w for grounded and 3w for non-grounded impedance) for extraction of signals proportional to the current through  $u_i$  and voltage  $u_u$  across the measured impedance  $Z_x$ ,
- the use of the SoC microsystems for harmonic excitation signal generation and orthogonal parts determination of signals  $u_i$  and  $u_u$ ,
- the use of the newest-generation microcontroller AVR32, which controls internal analyzer circuits: D/A and A/D converters, analog switches with the aid of I2C and SMI interfaces and communicates with the controlling PC via USB interface or UART and the connected ZigBee module.

The most important solution used in an advanced functionality analyzer is presented below.

J. Hoja, G. Lentka: THE FAMILY OF NEW GENERATION MINIATURIZED IMPEDANCE ANALYZERS ...

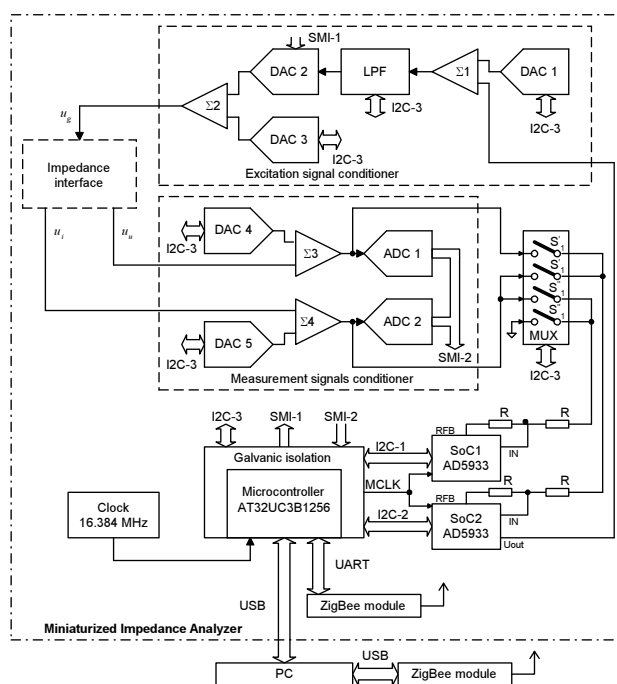


Fig. 3. Block diagram of the family of impedance analysers.

### 3.1. Non-grounded object impedance interface

The impedance interface for non-grounded impedance is based on a current-to-voltage converter (amplifier A1 in Fig. 4), which allows signal  $u_i$  proportional to current  $i_x$  flow through  $Z_x$  extraction. The extortion of virtual ground in point L and connection of ground G to the measured object  $Z_x$  shield allows to eliminate the influence of the parasitic capacitance existing between terminal L and the shield. To assure a wide range of measured impedance  $Z_x$  (current  $i_x$  changes from 10 pA up to 10 mA), eight range resistors  $R_R$  (100 M $\Omega$ , 10 M $\Omega$ ...10  $\Omega$ ) switched in decades have been used. Simultaneously with measurement range change ( $R_R$ ), resistors  $R_o$  ( $R_o = 0.1 R_R$ ) limiting the maximal current flowing to the current-to-voltage converter are switched.

The gain of amplifier A1, assuming a correctly chosen range resistor  $R_R$ , is not greater than 0.1, so the current-to-voltage converter output signal is additionally amplified  $\times 10$  using amplifier A5. In this way, the signal  $u_i$  amplitude is comparable to voltage  $u_u$  amplitude. Signal  $u_u$  is obtained from the measured impedance  $Z_x$  using voltage followers A2 and A4 and differential amplifier A6 (with unity gain).

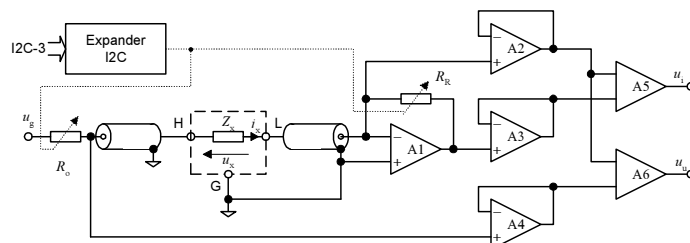


Fig. 4. Simplified schematic of the impedance interface for non-grounded impedance measurement.

### 3.2. Grounded object impedance interface

Figure 5 presents the developed impedance interface designed for impedance measurement of grounded objects. Range resistor  $R_R$  is connected in series with the measured impedance  $Z_x$  and switched in decades.  $R_R$  is used for measurement of current flow through  $Z_x$  with the aid of voltage followers A1, A2 and differential amplifier A5 with gain equal to 10. The values of range resistors  $R_R$  are identical as in the impedance interface for non-grounded objects, for a specific measurement range of  $Z_x$ . Signal  $u_i$  is taken from  $Z_x$  using voltage followers A3, A4 and differential amplifier A6 with unity gain.

The parasitic capacitance between terminals H and G is on the level of a dozen pF and is mainly caused by the capacitance of shielded cables and input capacitance of voltage followers A2 and A3. When we connect the signal from terminal H, with the aid of voltage follower A3 to the shield of cables, the meaningful elimination of the influence of parasitic capacitance on the result of impedance  $Z_x$  measurement can be observed.

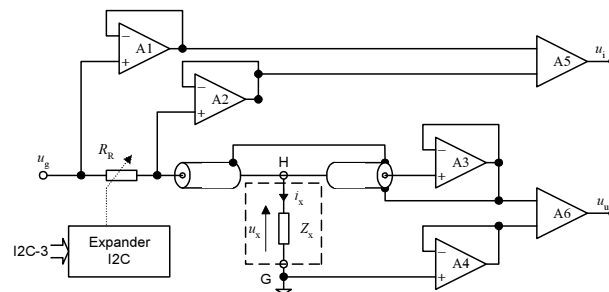


Fig. 5. Simplified schema of the impedance interface for grounded impedance measurement.

### 3.3. Excitation and measurement signal conditioners

At the input of the excitation signal conditioning path, DC offset is removed from the sinusoidal excitation signal, using amplifier ( $\Sigma 1$ ) and D/A converter (DAC1). Next, the signal is filtered in one of the seven switched low-pass filters (LPF) with bandwidths: 200 kHz, 20 kHz, 0.2 Hz. The amplitude of the excitation signal  $u_g$  can be programmed using multiplying D/A converter (DAC2). Finally, the excitation signal can be sourced with DC offset added using amplifier ( $\Sigma 2$ ) and D/A converter (DAC3).

The conditioner of measurement signals  $u_i$  and  $u_u$  contains two identical paths. Each of them uses D/A converters (DAC4 and 5) and amplifiers ( $\Sigma 3$  and 4) eliminating DC offsets from both signals, because usually DC offsets are much greater than the AC signal amplitude. This allows correct work of A/D converters of harmonic signals in SoC microsystems. For controlling the DC offset in the excitation signal and the measurement of DC offset in signals  $u_i$  and  $u_u$ , A/D converters (ADC1 and 2) have been used allowing the required DC polarization of the measured object.

### 3.4. The microcontroller-based controller with SoC microsystems

Energy-efficient SoC microsystems AD5933 [15, 16] have been used in the analyzer for extraction of orthogonal parts (Re and Im) of measurement signals  $u_i$ ,  $u_u$ . AD5933 integrates a sinusoidal signal generator and a measurement signal orthogonal parts extraction channel using the DSP technique. The sinusoidal signal generation (output  $u_{out}$ ) is performed on the basis of direct digital frequency synthesis (DDS). The generator consists of a 27-bit DDS

core, D/A converter and programmable gain and output resistance  $R_{out}$  amplifier. The measurement signal path consists of an input amplifier with gain defined by external resistors  $R$ , connected to terminals RFB and IN, amplifier with selected gain:  $\times 1$  or  $\times 5$ , antialiasing filter and 12-bit A/D converter. Calculation of parts: real (Re) and imaginary (Im) of the signal is performed by a hardware Discrete Fourier Transform (DFT) module on the basis of acquired signal samples. SoC is equipped with an I<sup>2</sup>C interface which is used for SoC control and readout of internal registers (e.g. Re and Im parts registers).

The AD5933 manufacturer does not assure the possibility of driving two SoCs with common I<sup>2</sup>C bus, because the SoC I<sup>2</sup>C address is identical for all chips (due to this fact, in the analyzer, two separate buses I2C-1 and I2C-2 have been used, one for each SoC). Moreover, there is no full synchronous generation of the excitation signal in relation to the clock signal MCLK. When analyzing the distribution of the MCLK signal inside the AD5933, one can note that the frequency divider providing signal clocking DDS generator (its memory contains a sample table approximating the generated sinusoidal signal) can cause an uncontrolled phase shift of the excitation signal  $u_{out}$ . The performed tests of the AD5933 showed that the lack of synchronization causes error in the determination of orthogonal parts (Re, Im) of the measurement signal in the SoC microsystem, which does not use the own generated excitation signal [17, 18]. This unwanted phenomenon is especially visible in the range of the highest measurement frequencies 10 kHz – 100 kHz.

Due to this fact, in the frequency range 100 Hz – 100 kHz, the orthogonal parts of signals  $u_i$  and  $u_{ii}$  are determined sequentially by the SoC2 microsystem (switched by Mux). In this frequency range, measurement time is on the level of tens ms and affects the impedance spectrum total acquisition time only a little. But for low frequencies below 100 Hz, simultaneous measurement of orthogonal parts of signals  $u_i$  and  $u_{ii}$  has been used with the aid of both SoC1 and SoC2 microsystems. These solutions have allowed meaningful (ca. twofold) shortening of impedance spectrum measurement time.

The analyzer controller has been based on an energy-efficient 32-bit microcontroller from the AVR32 family (AT32UC3B1256) working under RTOS-based software. It realizes communication with the PC via an USB interface or UART interface and a ZigBee module. The controller controls other modules: configures measurement paths, sets generated excitation signal parameters and parameters of measurement signals  $u_i$  and  $u_{ii}$ .

When using its internal clock source, the AD5933 allows sinusoidal signal generation in the range of 1 kHz – 100 kHz. For impedance spectroscopy, the required measurement frequency range is much wider. In order to achieve impedance spectrum measurement in a frequency range of 10 mHz – 100 kHz in the developed analyzers, an external clock source was used (16.384 MHz) as well as programmable frequency dividers in the microcontrollers, providing the external clock signal MCLK for SoCs. Table 1 presents parameters of the generated signal in the SoC2 microsystem and the number of periods ( $L$ ), in which the samples are acquired depending on the MCLK frequency.

Table 1. Measurement signal parameters.

$f_{MCLK}$ [Hz]	$f_{meas}$ [Hz]	Step $\Delta f_{meas}$ [Hz]	Number of periods $L$
16.384 M	10 k – 100 k	10 k	10–100
1.6384 M	2 k – 9 k	1 k	20–90
1.6384 M	200 – 1 k	100	2–10
163.84 k	20 – 100	10	2–10
16.384 k	2 – 10	1	2–10
1.6384 k	0.2 – 1	0.1	2–10
163.84	0.02 – 0.1	0.01	2–10
81.92	0.01	–	2



The microcontroller calculates modulus and argument of the measured object impedance, on the basis of measurement signal orthogonal parts determined by AD5933 microsystems according to formulas:

$$|Z_x| = \sqrt{\frac{(\operatorname{Re}U_u)^2 + (\operatorname{Im}U_u)^2}{(\operatorname{Re}U_i)^2 + (\operatorname{Im}U_i)^2}} R_R, \quad \varphi_{Z_x} = \arctan \frac{\operatorname{Im}U_u}{\operatorname{Re}U_u} - \arctan \frac{\operatorname{Im}U_i}{\operatorname{Re}U_i}, \quad (1)$$

where  $R_R$  – range resistance;  $\operatorname{Re}U_u$ ,  $\operatorname{Im}U_u$ ,  $\operatorname{Re}U_i$  and  $\operatorname{Im}U_i$  – orthogonal parts of signals  $u_i$  and  $u_u$  read from SoC registers.

#### 4. Impedance Analyzers Construction

The impedance analyzers were realized in module form, depending on version on 4 or 5 PCB packets with 65×80 mm dimension, using SMD technology (except range resistors with 0.1% tolerance). The packets were designed to be located in a sealed case. The construction was divided into functional blocks (realized on separate packets) according to the block diagram presented in Fig. 3. The following packets: excitation signal conditioner (GEN), measurement signals conditioner (ADC), microcontroller based controller (MAIN) and two versions of impedance interface (3w – OWSY, 2w – OWUZ) were designed.

The analyzer, powered and controlled via an USB interface, consists of 4 packets: GEN, ADC, MAIN and OWSY or OWUZ depending on the tested object (grounded or non-grounded).

The analyzer with built-in accumulator battery and wireless communication is shown on the photography (Fig. 6). This analyzer, besides the above mentioned packets, contains an additional packet (with dimensions 65×120 mm) responsible for ZigBee communication between the analyzer and the controlling PC.

The analyzer in a basic configuration (shown on photo in Fig. 1) has separate packets of replaceable impedance interfaces, but other blocks were integrated into one packet.

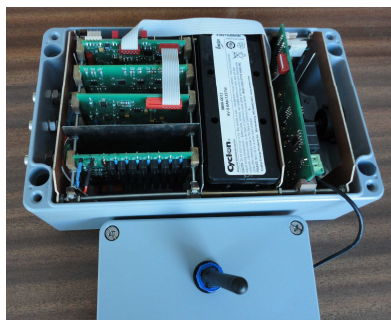


Fig. 6. View of internal construction of the analyzer with wireless communication.

#### 5. Impedance measurement using the realized analyzer

Tests have been performed in order to evaluate the accuracy of the impedance modulus and argument measurement, dependent mainly on impedance interface and SoC microsystems determining the orthogonal parts of signals  $u_i$ ,  $u_u$ . The 4-element reference two-terminal RC network was used as a test object with component values as follows:  $C_c = 184.7$  pF,  $R_p = 497.09$  MΩ,  $R_{cr} = 988.82$  MΩ and  $C_{dl} = 4.39$  nF. The object represents a typical equivalent circuit of an anticorrosion coating at a stage when the undercoating rusting begins.

The capacitors were measured using Precision LCR Meter E4980A, but resistors were measured using the technical method with the aid of reference resistor and HP34401A multimeter.

To compare the accuracy of orthogonal parts determination using SoC microsystems with traditional solution using phase-sensitive detectors, the measurements have been performed using a laboratory vector voltmeter FRA1255 from Solartron. When measuring with FRA1255, the FRA signal generator was applied instead of signal  $U_{out}$  from SoC2, and signals  $u_i$ ,  $u_u$  from Mux were connected to inputs of the two-channel vector voltmeter.

To control test measurements, the dedicated graphic user interface (GUI) was designed as shown in Fig. 7. The software allows manual setting of all parameters of the analyzer paths and SoC microsystems when the analyzer works standalone as well as when connected to FRA1255. The GUI allows to read determined orthogonal parts of signals from SoC microsystems and impedance parameters  $|Z_x|$  and  $\arg Z_x$  calculated by the microcontroller at selected measurement frequencies. The GUI also presents the impedance spectrum of the tested two-terminal RC network on Bode plots in a frequency range of 10 mHz – 100 kHz. The spectrum curvature shows that the tested RC network allows the analyzer evaluation in different measurement conditions: for  $Z_x$  modulus changing from several k $\Omega$  up to 1 G $\Omega$ , and for  $Z_x$  argument changing from  $-90^\circ$  at high frequencies (the  $C_c$  capacitance dominates in the object) down to  $-10^\circ$  at low frequencies (the sum of  $R_p$  and  $R_{ct}$  dominates in the object).

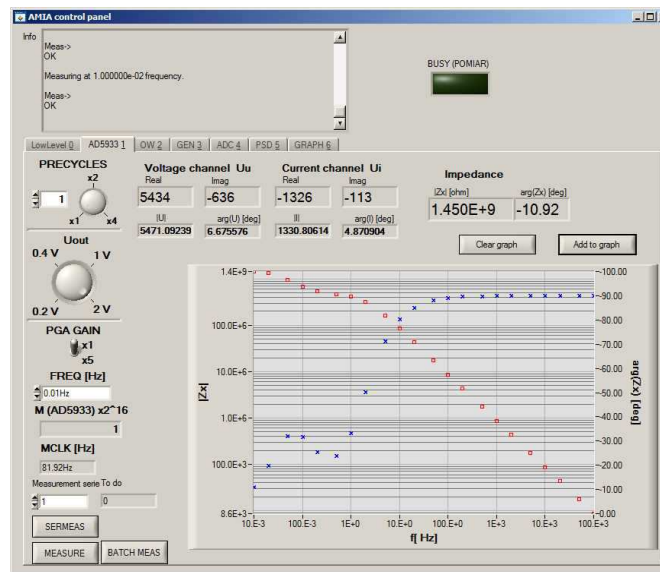


Fig. 7. View of the graphic user interface for testing the developed analyzers with results of measurement in the form of Bode plots (the impedance module (o) and the impedance argument (x)).

The RC two-terminal network impedance measurements have been performed in the frequency range of 10 mHz – 100 kHz at 3 frequency points (using 1-2-5 steps) in each decade. For each frequency, 10 measurement series were performed, and calculated mean values were compared with values calculated theoretically on the basis of reference values of RC network components. Fig. 8 presents the relative error of the impedance modulus and the absolute error of impedance argument of the RC two-terminal network for measurement with the developed analyser and with FRA1255 connected to the measurement paths of the analyzer.



*Metrol. Meas. Syst.*, Vol. XX (2013), No. 1, pp. 43–52.

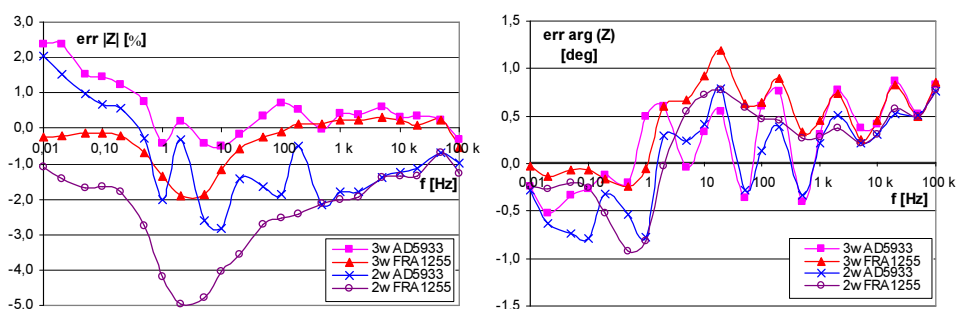


Fig. 8. Relative error of the impedance modulus and absolute error of impedance argument of the tested object for grounded objects interface (2w) and non-grounded objects interface (3w).

When analyzing graphs of errors of modulus and argument of impedance, one can note the following conclusions:

- Grounded impedance measurements (2w) are obtained with a greater impedance modulus error (for frequencies greater than 1 Hz), caused by incomplete parasitic capacitance compensation in the impedance interface (e.g. capacitance of shielded cables, input capacitance of the voltage follower).
- Errors of impedance modulus for the analyser with orthogonal parts determined by AD5933 and for phase-sensitive detectors in FRA1255 are at a similar level (for frequencies greater than 100 Hz).
- In the case of AD5933, a much greater, cyclic change of impedance argument error can be noticed in each measurement range. Just before a change of the range resistor  $R_R$  to a higher value, the error has the greatest value, because measurement signal  $u_i$  has the smallest amplitude and the influence of the resolution of the 12-bit A/D converter in AD5933 can be observed.
- Impedance modulus error increases for lower frequencies (<1 Hz) in case of AD5933 but in case of FRA1255, the error increases in the frequency range of 1 Hz – 10 Hz where the real and imaginary parts of impedance of the tested two-terminal RC network are comparable. The existing differences result from the use of different methods for determination of the orthogonal parts of signals  $u_i$  and  $u_u$  in AD5933 and in FRA1255.

Resuming, the obtained accuracy of the impedance modulus and argument measurement using the developed analyzers are fully acceptable in case of measurements in the field.

## 6. Conclusions

The innovative features of the developed new generation of impedance spectroscopy analyzers are miniaturization, low power consumption, low cost, possibility of controlling and powering the instrument via an USB interface, as well as wireless communication. The developed instrumentation can be characterized by metrological parameters comparable to similar portable instruments offered by top worldwide manufacturers (Gamry, Ivium):

- Impedance measurement range:  $10 \Omega < |Z_x| < 10 \text{ G}\Omega$  (in 8 subranges).
- Frequency range of impedance spectroscopy: from 10 mHz up to 100 kHz (10 frequency points in each decade).
- Measurement signal amplitude programmable in the range of 1 mV–1 V (with 1 mV step), the amplitude is automatically regulated on the programmed level when changing the frequency and impedance measurement ranges.
- DC offset set in the range  $\pm 4 \text{ V}$  with 1 mV step, allowing automatic compensation of object free-potential or extorts the required DC polarization on the tested object.

J. Hoja, G. Lentka: THE FAMILY OF NEW GENERATION MINIATURIZED IMPEDANCE ANALYZERS ...

- The analyzers are powered by a DC voltage of 5 V taken from the USB or built-in accumulator battery, the power consumption is lower than 1.5 W.
  - In case of necessity of extending the distance from the analyzer to the controlling computer above 5 m, an alternative analyzer version was developed (in a slightly bigger case) with wireless telemetry on the basis of ZigBee with own built-in accumulator power.
- The developed family of miniaturized impedance analyzers can fill the existing gap on the worldwide market of impedance spectroscopy instrumentation, where is a lack of low-cost, miniaturized, field-worthy instrumentation. All analyzer versions are technologically advanced and can be quickly turned into medium-volume production.

### Acknowledgements

This work was supported by the National Centre for Research and Development, Poland (grant # NR01-0051-10/2010).

### References

- [1] Barsoukov, E., Macdonald, J.R. (2005). *Impedance Spectroscopy: Theory, Experiment and Applications*. John Wiley & Sons.
- [2] Srinivas, K., Sarah, P., Suryanarayana, S.V. (2003). Impedance spectroscopy study of polycrystalline  $\text{Bi}_6\text{Fe}_2\text{Ti}_3\text{O}_{18}$ , *Bulletin of Material Science*, (26), 247–253.
- [3] Skale, S., Doležek, V., Slemnik, M. (2008). Electrochemical impedance studies of corrosion protected surfaces covered by epoxy polyamide coating systems. *In Prog. Organic Coat.*, (62), 12, 2456–2460.
- [4] Xu, Z., Neoh, K.G., Kishen, A. (2008). Monitoring acid-demineralization of human dentine by electrochemical impedance spectroscopy. *Journal of Dentistry*, 36(12), 1005–1012.
- [5] Uchiyama, T., Ishigame, S., Niitsuma, J., Aikawa, Y., Ohta, Y. (2008). Multi-frequency bioelectrical impedance analysis of skin rubor with two-electrode technique. *J. of Tissue Viability*, 17(4), 110–114.
- [6] Macdonald, J.R. (1999). *LEVM Manual v.7.11. CNLS Immittance Fitting Program*. Solartron Group Ltd.
- [7] ZPlot for Windows, Electrochemical Impedance Software, Ver. 1.2, Operating Manual, Scribner Assoc. Inc., Charlottesville, Virginia 1995.
- [8] Solartron Analytical (2005). 1260 Impedance/gain-phase Analyzer. Operating Manual.
- [9] Agilent Technologies (2003). Agilent 4294A Precision Impedance Analyzer, Operation Manual.
- [10] Novocontrol, ALPHA Series Analyzer (Dec. 2012). [http://www.novocontrol.de/html/index\\_analyzer.htm](http://www.novocontrol.de/html/index_analyzer.htm)
- [11] Gamry Instruments, Reference 600 Potentiostat/Galvanostat/ZRA Operator's Manual (Dec. 2012) <http://www.gamry.com/assets/Uploads/Reference-600-Operators-Manual.pdf>
- [12] Ivium, Ivium Compact Stat (Dec. 2012). <http://www.ivium.nl/CompactStat>
- [13] ATLAS 0441 High Impedance Analyser (Dec. 2012). <http://www.atlas-sollich.pl/eng/products/0441.htm>.
- [14] Bordzilowski, J., Darowicki, K., Krakowiak, S., Krolikowska, A. (2003). Impedance measurements of coating properties on bridge structures. *Progress in Organic Coatings*, 46, 216–219.
- [15] Analog Devices (2005). AD5933 1 MSPS, 12-Bit Impedance Converter, Network Analyzer.
- [16] Analog Devices (2005). Evaluation Board for the 1 MSPS 12-Bit, Impedance Converter Network Analyzer, Preliminary Technical Data EVAL-AD5933EB.
- [17] Hoja, J., Lentka, G. (2009). Portable analyzer for impedance spectroscopy. *In Proc. XIX IMEKO World Congress Fundamental and Applied Metrology*, Lisbon, Portugal, 497–502.
- [18] Hoja, J., Lentka, G. (2010). Interface circuit for impedance sensors using two specialized single-chip microsystems. *Sensors and Actuators A-physical*, 163(1), 191–197.
- [19] Hoja, J., Lentka, G. (2007). The limitations of virtual impedance meter based on a data acquisition card. *Measurement Automation and Monitoring*, 53(9bis), 657–660.